Journal of Applied Sciences

ISSN 1812-5654

science alert

ANSInet
an open access publisher
http://ansinet.com

Journal of Applied Sciences 15 (1): 32-45, 2015
ISSN 1812-5654 / DOI: 10.3923/jas.2015.32.45

Combined Use of Electrical and Flow Parameters for Hydrogeological Characterization of Piedmont Aquifers in the Basement Complex

[1]Etienne Leonel Amougou Menkpa, [2]Philippe Njandjock Nouck,
[1]Joseph Quentin Yene Atangana and [1]Joseph Mvondo Ondoua
[1]Unit of Formation and Doctoral Research Geosciences and Applications,
[2]Unit of Formation and Doctoral Research Physics and Applications,
University of Yaounde I, P.O. Box 812, Yaounde, Cameroun

Abstract: This study is an attempt to clarify and understand the structure of the basement, aquifer behavior and to determine the parameters that influence the productivity of drillings in the piedmont region in the Far North of Cameroun, with the optics to guide future hydraulic campaigns in similar regions of the World. The data used are the vertical electrical soundings collected during geophysical surveys and parameters identified during the drilling works. The analysis and the interpretation of qualitative and quantitative data have highlighted terrain models and two types of aquifer, one on the surface alluvium and another in the deep aquifer of the fissured/factured basement horizons. The statistical analysis of the boreholes productivity has permitted to conclude that: the depth of drilling is not the guarantee of a high flow rate; in the alluvium or alterite formation, they flow rate increases with the thicknesses between 1 to 35 m and decrease for higher thicknesses; while in fissured aquifer significant water arrivals are only observed in the first 15 m of the fissured/fractured rock; The extreme variability of flows observed around neighboring boreholes, emphasizes the discontinuous nature of these aquifers.

Key words: Aquifers behavior, electrical survey, hydrogeological characterization, drilling productivity, piedmont

INTRODUCTION

Several efforts in the world are made by the public services to manage the urban, periurban and rural centers in quality water through several programs from national and international partnerships. However, difficulties exist since portable water is still unavailable for everyone. The supply of portable water is thus oriented towards the research for underground water, whose qualities generally fulfill the international norms of the OMS (Faillat, 1986; Biemi, 1992; Abe-Sombo *et al*., 2011). The necessity to urgently and immediately satisfy the need for water of the populations in regions with hydric deficits in quality water leads to a precipitation in the realization of borings. Generally, these works realized on the bases of geomorphological considerations are no longer useable in long term due to their frequent dry up. Thus contributing to less water supply and consequently, scarcity in potable water in cities and villages especially during drought and hence a waste in finance.

The aim of this work is to understand the electrical and mechanical behavior of the aquifers of piedmont, all this by specifying the underground structure of aquifers and to determine the parameters susceptible to influence the productivity of borings, with a view to generalize this information for the guidance of hydraulic campaigns in similar regions. To this effect, the use of vertical electrical sounding data from the application of the electrical method of Schlumberger (Atangana, 1992; Robain *et al*., 1996; Teikeu *et al*., 2012a; Nouck *et al*., 2013), combined with data from drilling parameters (lithological logs, total drilled depth, thickness of weathered level, static level, depth of water inflow, flow), appear to be very interesting for hydrogeological characterization of aquifers in this context.

MATERIALS AND METHODS

Geologic and geographic settings of the study area: The study area also called the piedmont area is located between the mountainous area of the Mandara Mountains and the vast plains of the Logone and Chari field (Detay, 1987). It is locally dominated by Quaternary alluvial mantles named «comblement Tchadien» meaning

Corresponding Author: Philippe Njandjock Nouck, Unit of Formation and Doctoral Research Physics and Applications, University of Yaounde I, P.O. Box 812, Yaounde, Cameroun

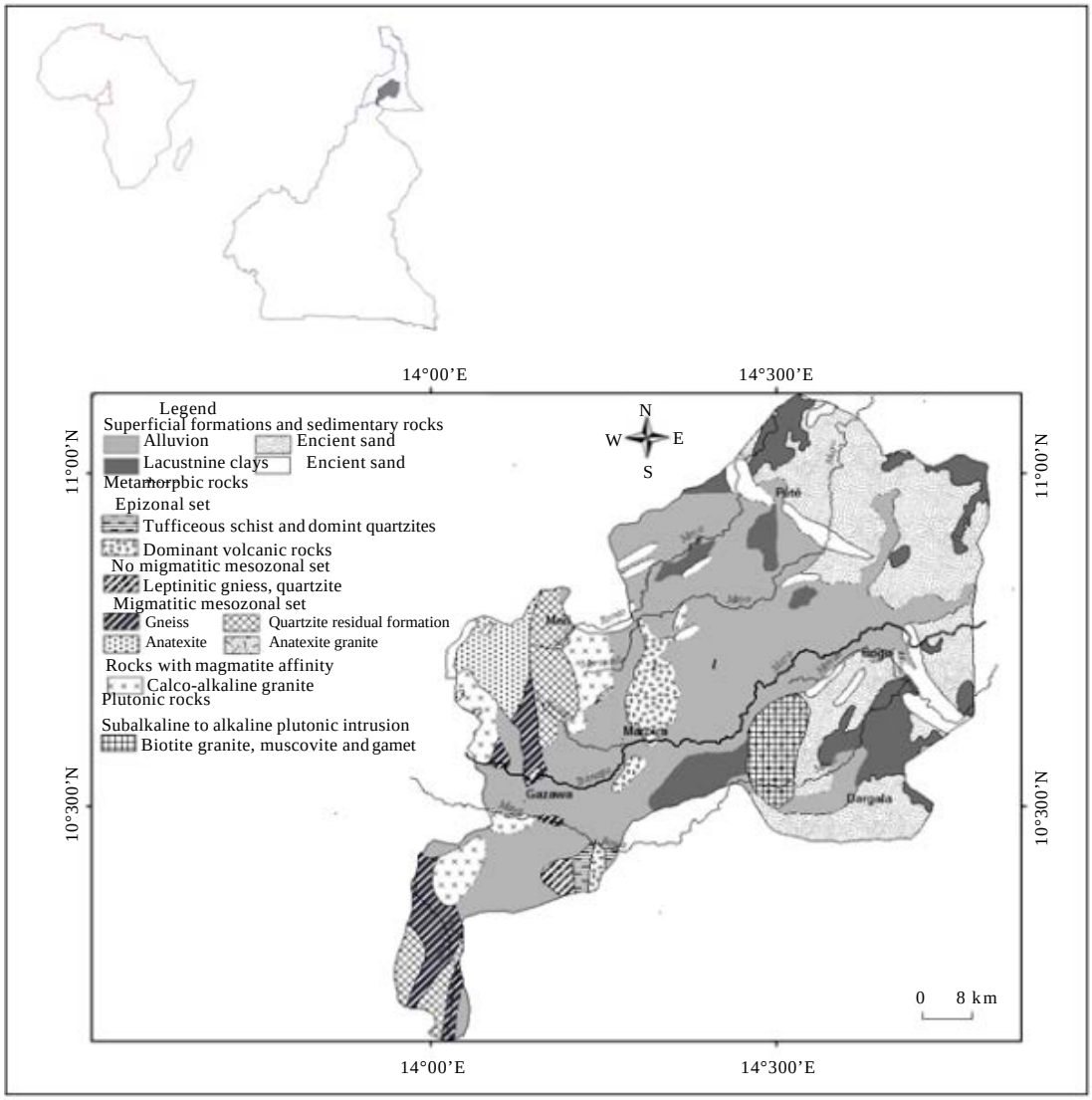

Fig. 1: Geologic map of the study region

Tchadian fill up and ancient Tchadian continental terminal sands. They are detrital arenas and less evolved lithosols which mask the original geologic formations. Petrographic studies in the area revealed a Precambrian crystalline basement, made on one hand by original metamorphic formations of epizonal formation (metavolcanites, tufaceous schists and dominant quartzites); non migmatitic mesozonal formations (leptinitic gneiss and quartzite); migmatitic mesozonal formations (embrechitic-gneiss, anatexis granite) and on the other hand, by formations of migmatitic affinity (calco-alkaline granites) and plutonic formations, two-mica (biotite and muscovite) and garnet granites which outcrop as domes in some places (Fig. 1).

This region is located in the Far-North of Cameroon between latitudes N10°9' and 11°6' and longitudes E13°56' and 14°48' called Diamaré, the region occupies a surface area of about 4818 km^2. It has a dry tropical climate, characterized by high average annual temperatures (27.7°C) and two well distinct seasons. The average annual rainfall varies between 1000 mm in the Mandara mountains to 500 mm in the "Yaérés" plains. The registered absolute minimal temperature is 11.4°C against an absolute maximal temperature of 45.5°C

(Ngoupayou, 1997). These climatic parameters are actually influenced by climate change phenomena and contribute to high water evaporation, drying up of streams and soils, desert advancing, leading to water scarcity in certain periods of the year (Zakari *et al*., 2014).

Data and methodology: Geophysics is an appreciable instrument in the guide for hydrogeological research programs, whether in the identification of new resources or in the amelioration of knowledge concerning a reservoir aquifer. The electrical method, through the Schlumberger lateral (electrical dragging) and vertical (electrical sounding) investigation techniques were applied in this study. This is because it seems to be the most adapted, due to the fact that it is light, its high credibility and favorable geological setting consists of lithologic formations having different resistivity priori (Lachassangne *et al*., 1996). This method is based on the injection of electric current into the ground and intensity (I) at the surface, at mid distance between the two emission electrodes (A and B). This dispositive is followed by the measurement of the potential difference (V), created by current flow through the crossed formations at the middle of the reception electrodes (M and N). This is aimed to establish apparent resistivity variation curves (ρ_a) with respect to the distance AB/2 (Teikeu *et al*., 2012b; Nouck *et al*., 2013).

According to Telford *et al*. (1990), for a homogeneous field and isotope:

$$\Delta V_{MN} = \frac{1}{2\pi}\left(\frac{1}{AM} - \frac{1}{AN} - \frac{1}{BM} + \frac{1}{BN}\right)\rho I \quad (1)$$

This Eq. 2 allows us to deduce the true resistivity:

$$\rho = K\frac{\Delta V}{I} \quad (2)$$

With:

$$K = \frac{2\pi}{\frac{1}{AM} - \frac{1}{AN} - \frac{1}{BM} + \frac{1}{BN}} \quad (3)$$

The factor K given by Eq. 3 is called “Geometrical factor” and depends only on the relative position of the four electrodes. It is calculated from the lengths in meters.

If the field is not homogeneous, obtained from K, ΔV and I apparent resistivity ρ_a linked by complex relationships with true resistivities and thicknesses of all layers influenced by the AMNB measuring device.

It consists of revealing the underground geologic discontinuities that are potentially associated to water transfer (Meli'i *et al*., 2011; Nkoungou *et al*., 2012). According to Seladji *et al*. (2007) the measured resistivity decreases when water content and degree of saturation increases. The water content and electric resistivity ratio constitutes a major advantage for electrical resistivity methods in the search for underground waters. Darcy's law assumes a linear relationship between flow and pressure drop through a porous medium and show that, the load can be seen as the potential of the flow velocity field at each point M = (x, y, z) of the space greater than that of gravel or crack scales.

The porosity P of a porous medium is given in Eq. 4:

$$P = \frac{V(\text{Total volume of pores})}{V(\text{Total volume})} \quad (4)$$

The specific surface area S is given by Eq. 5:

$$S = \frac{S(\text{Total surface of pores})}{V(\text{Total volume of a sample})} \quad (5)$$

From the Eq. 5 the effective porosity n_e can be obtained with Eq. 6:

$$n_e = \frac{V(\text{Volume of water that can circulate})}{V(\text{Total volume of sample})} = \frac{\text{Darcy speed}}{\text{Water speed}} \quad (6)$$

The storage capacity Sc for a porous medium can be expressed by Eq. 7:

$$S_c = \frac{\text{Specific yield}}{V(\text{Total volume of sample})} \quad (7)$$

In the porous medium, the gradient load or hydraulic gradient can be expressed by Eq. 8:

$$\frac{\Delta h}{L} \quad (8)$$

where, Δh is loss load between the top and bottom of the porous medium and L, the thickness of the porous medium.

According to Darcy law, the flow rate through the porous medium Q is given by Eq. 9:

$$Q = K.A.\frac{\Delta h}{L} \quad (9)$$

where, K is the permeability and A the normal section of this porous medium.

Hydrogeological characterization of aquifers also requires the implementation of a tool whose results are complementary to those of the electrical method. It is in this context that a statistical analysis to assess the influence of parameters on the flow rates of drill works was used. For this, the correlation coefficients (r) (Pearson, 1895) between flow (Q) and various mechanical parameters (y) from the covariance between Q and y (σ_{Qy}) and standard deviations of Q and (σ_y) were calculated by applying Eq. 10-13:

$$r_{Q,y} = \frac{\sigma_{Qy}}{\sigma_Q \sigma_y} \quad (10)$$

with:

$$\sigma_{Q,y} = \frac{\sum_{i=1}^{N}(Q_i - m_Q)(y_i - m_y)}{N} \quad (11)$$

$$\sigma_Q = \sqrt{\frac{\sum_{i=1}^{N}(Q_i - m_Q)^2}{N}} \quad (12)$$

and:

$$\sigma_y = \sqrt{\frac{\sum_{i=1}^{N}(y_i - m_y)^2}{N}} \quad (13)$$

where, N is the total number of wells whose flow rates were measured, m_Q and m_y are averages Q and y.

All these analyses highlight the links or absence of links between the evolutions of the different parameters.

In this study, according to Eq. 1, 2 and 3, 56 vertical electrical sounding (SEV) of the Schlumberger type, were collected in the field using the Syscal IRIS Instrument electrical resistivity device with the wire lengths ranged from 1.5 -120 m to the distance AB/2 and 0.5, 1.5, 2.5, 5.0, 10.0 and 15.0 m for the different distances of MN/2. Also, The Géo.Elect.Mod software was used in the interpretation of electrical sounding from Gosh linear filters combined with parameters of 68 wells (boreholes) and their drill (Fig. 2).

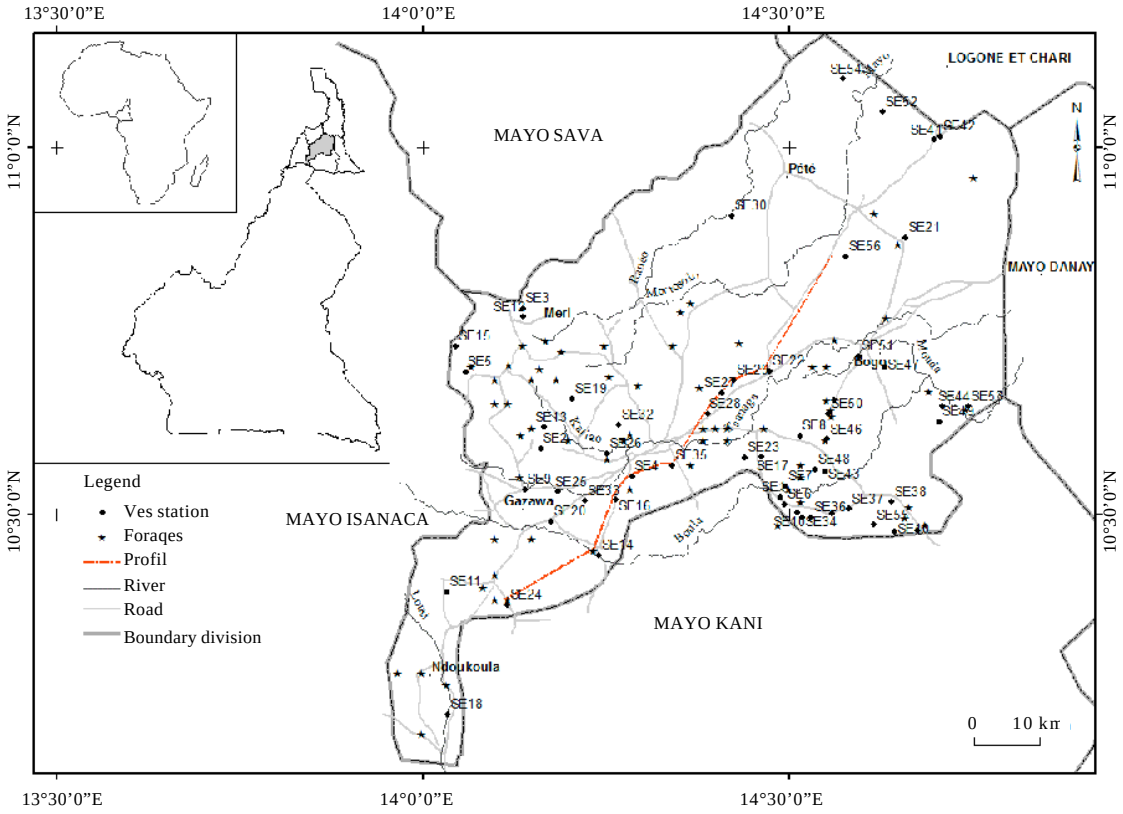

Fig. 2: Map of study area showing electrical drills and well locations

RESULTS AND DISCUSION

Sounding curves: According to the data collected during the framework and using Eq. 2, the sounding curves was summarized into seven categories (Table 1), inspired from those realized by Koussoube *et al.* (2003), Abe-Sombo *et al.* (2011), Teikeu *et al.* (2012a) and Nouck *et al.* (2013).

Curves of H, HA and QH type: These curves present the form of a «boat base» with symmetric (Fig. 3a) or asymmetric (Fig. 3b, c) branches. It does not give any indication that can clarify the presence of fractures. These fractures are actually present but are often masked at the base of alterites or are mistaken for basements due to itssmall thickness at greater depths (Koussoube *et al.*, 2003). The interpretation of these curves (Table 2), shows a structure with three geo-electrically distinct layered terrains with respect to the behaviour of the curve's branches. The descending branch characterizes a resistant autochthonous clayey sand lateritic layer (in the basement zone) or allochthonous sandy clay layer (in the alluvial or sandy zone). Its resistance is due to climatic conditions and represents the superficial Arable recover with a relatively small thickness of 0.5-3 m. The conducting aquifer complex with an average thickness of 15-25 m is represented by the boat base like point and the starting points of the ascending walls and is associated to the residual clayey sand weathering or sandy strata of an alluvial clayey episode. Its resistivity is relatively weaker than that of the upper layer due to its high water content, covering a confined aquifer in the lateritic zone or the unconfined aquifer (phreatic nap) in the alluvial zone. The ascending branch is characteristic to the laterite's parent rock or a resistant colluvial arena (Fig. 3d).

Curves of KH type: With this type of curves, four terrains can be distinguished (Table 2). They have "Bell and boat base-like" forms (Fig. 4a) and are characteristic to zones where cuirassed or ferruginous gravels were formed, just after the autochthonous clayey or allochthonous silty sand lateritic superficial cover. On the profile, it is the second layer of the terrain and is more resistant than the first layer, thus giving the curve a "Bell-like" shape. The other terrains are the same as those defined by a "Boat base like" form. On the hydrogeological point of view, they signal a single localizable confined aquifer in the alterite or in the weathering front of the fissured/fractured parent rock (Fig. 4b).

Curves of HH type: They present a curve with a «two consecutive boat base-like» forms (Fig. 5a) and

Table 1: Station location and curve types

VES stn	Longitudes	Latitudes	Curve types	Nom	Longitudes	Latitudes	Curve types
SE1	14.4888	10.52305	H	SE29	14.42449	10.68313	KH
SE2	14.16138	10.58972	HA	SE30	14.42196	10.90592	QH
SE3	14.13722	10.78032	H	SE31	14.55885	105011	A
SE4	14.2861	1055138	HA	SE32	14.26806	10.62218	HH
SE5	14.05913	10.6935	H	SE33	14.22113	10.51836	A
SE6	14.49416	10.51362	H	SE34	14.51852	10.49577	HH
SE7	14.49561	10.53814	H	SE35	14.3406	10.5666	A
SE8	14.51502	10.60702	HH	SE36	14.53014	10.49627	H
SE9	14.13957	10.53421	HA	SE37	14.5814	10.50758	A
SE10	14.51094	10.50276	HA	SE38	14.64	10.517	H
SE11	14.03333	10.394722	HA	SE39	14.675	10.478	H
SE12	14.13749	10.76891	HA	SE40	14.644	10.477	H
SE13	14.16609	10.61836	A	SE41	14.69752	11.0101	QH
SE14	14.24	10.445	HA	SE42	14.70592	11.01504	H
SE15	14.04599	10.729	A	SE43	14.549	10.558	H
SE16	14.26406	10.52048	A	SE44	14.709	10.647	H
SE19	14.20388	10.65722	KH	SE45	14.56133	10.65575	QH
SE18	14.0352	10.22782	A	SE46	14.55218	10.60239	H
SE17	14.46206	10.57903	A	SE47	14.631	10.7	H
SE20	14.17609	10.49022	H	SE48	14.536	10.561	H
SE21	14.65867	10.87632	H	SE49	14.705	10.626	KH
SE22	14.47373	10.69475	H	SE50	14.55269	10.63709	H
SE23	14.43982	10.57727	HA	SE51	14.59562	10.7151	KH
SE24	14.11636	10.37672	A	SE52	14.628	11.048	KH
SE25	14.18495	10.5307	A	SE53	14.744	10.647	Q
SE26	14.25191	10.58229	A	SE54	14.57379	11.09238	Q
SE27	14.40897	10.66491	KH	SE55	14.616	10.486	HH
SE28	14.38895	10.63682	KH	SE56	14.57802	10.85106	HH

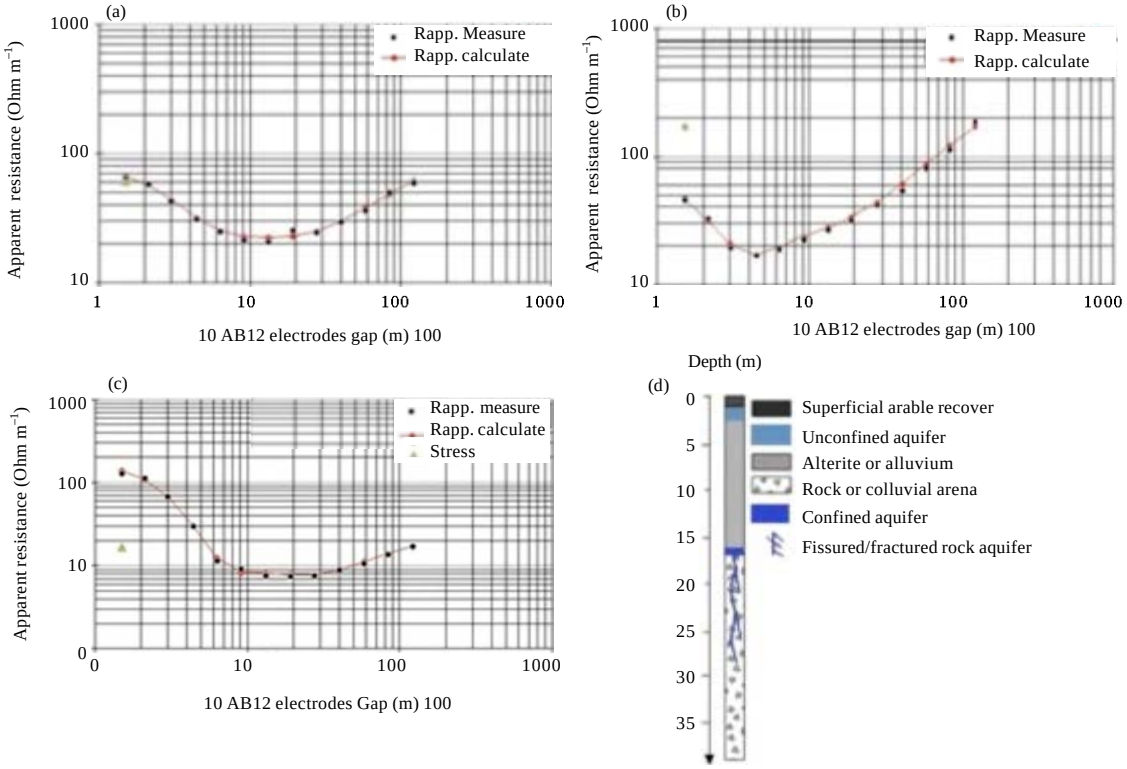

Fig. 3(a-d): Geoelectrical model and general shapes of type H, AH and QH curves

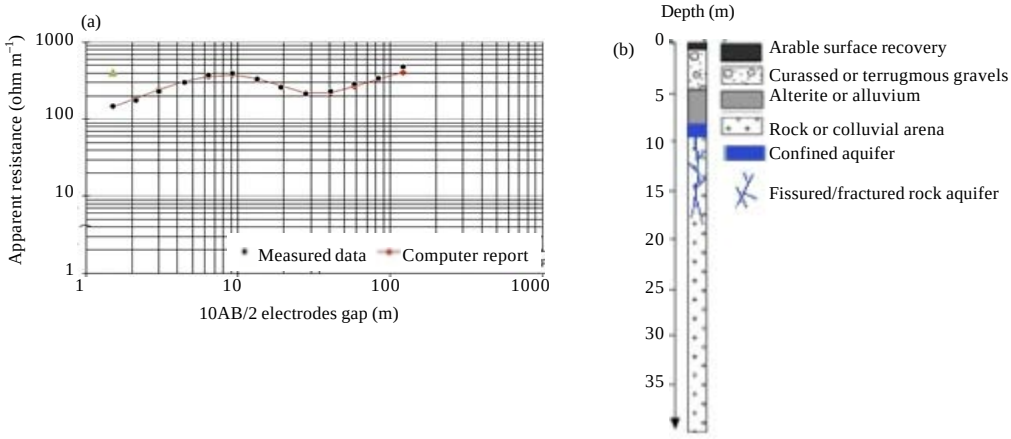

Fig. 4(a-b): Geoelectrical model and general shape of KH type curves

characterize terrain models with five layers (Fig. 5b). Their interpretation (Table 2) reveals two superposed aquifer levels: The first superficial aquifer is situated in the lateritic or alluvial superficial formation and is supplied by meteoric water and the infiltration of the neighbouring river "Mayo"; the second deep aquifer in the fissured basement and weathered or weathering front and supplied through underground fractures that are connected to the drainage network.

Curves of A and Q types: These are curves with a single descending branch (Q type) (Fig. 6a) or a ascending branch (A type) (Fig. 6c). They characterize terrain models with two or three layers when they are in a regular

Table 2: Geoelectrical parameters of VES stations

VES stn	Resistivity (Ωm)	Thickness (m)	VES stn	Resistivity (Ωm)	Thickness (m)	VES stn	Resistivity (Ωm)	Thickness (m)	VES stn	Resistivity (Ωm)	Thickness (m)	VES stn	Resistivity (Ωm)	Thickness (m)	VES stn	Resistivity (Ωm)	Thickness (m)
SE1	122	0.6	SE12	41	0.7	SE24	15	0.5		3.24	4.5		7	67.5	SE55	18	0.9
	71	7.2		5	1		7	1.7		9	11		85	/		4	1.2
	211	13.2		41	7.7		13	14.4		4192	/	SE43	50	0.6		28	2.7
	2679	/		9924	/		329	/	SE34	26	0.9		8	4.8		1	6.4
SE2	945	0.3	SE13	21	7.8	SE25	11	0.9		3	1.4		494	/		16	/
	40	9.4		27	21.4		7	8		73	6.9	SE44	55	0.5		51	0.8
	1867	/		84.72	/		3739	/		5	11.5		5	12.8	SE56	13	3.8
SE3	250	0.9	SE14	11	1.9	SE26	11	0.5		1327	/		271	/		5	3.6
	40	8		5	3		4	5.5	SE35	14	0.9	SE45	330	1.1		26	10.2
	6636	/		46	75.8		2461	21.4		11	4		43	8.1		2	22
SE4	240	0.4		1450	/	SE27	41	0.6		111	6.4		3801	/		915	/
	12	8.6	SE15	15	0.7		317	3.9		6	14.7	SE46	103	1.5			
	181	/		10	4.6		1	5.4		3801	/		29	11.3			
SE5	287	1.2		2?2	/		70	/	SE36	13	0.9		750	/			
	37	16.2	SE16	11	6.6	SE28	100	1.5		1	1.2	SE47	154	3.7			
	496	/		60	5.5		1655	2.4		38	3.5		20	14.1			
SE6	259	0.9		4155	/		281	6.1		4	19		556	/			
	17	7.7		34	1.6		20	3		729	/	SE48	443	0.9			
	1350	/		67	15.9		6910	/	SE37	10	1.2		38	10.8			
SE7	90	13	SE17	1121	/	SE29	86	0.3		7	3.5		5038	/			
	15	20		142	2.58		215	2.9		176	5.9	SE49	20	2.3			
	25	5		515	22.7		666	2.6		7	15.2		3	8.5			
	1570	/	SE18	2513	/		4	14		4478	/		2414	/			
SE8	46	1.1		103	1		240	/	SE38	481	0.5	SE50	15	0.7			
	22	4.8		2135	1.5	SE30	19	0.9		54	2.4		2	9			
	410	4.4		63	8.4		19	3.9		7	2.9		5630	/			
	59	24	SE19	849	/		33	55.4		27	38.3	SE51	17	0.7			
	960	/		251	0.4		138	/		3121	/		104	4.2			
SE9	75	0.9		30	1.2	SE31	19	0.9	SE39	206	0.7		7	6.3			
	6	1		16	16.9		11	0.8		18	6.5		119	/			
	32	16.6	SE20	4800	/		7	4		7	7.4	SE52	193	1.2			
	1855	/		36	0.9		89	10.5		4061	/		597	0.9			
SE10	61	1		5	29.7		12	19.4	SE40	77	1.3		32	19.9			
	8	1.4	SE21	97	/		5612	/		21	24.7	SE53	146	/			
	42	16.8		97	0.7	SE32	21	0.8		138	/		71	0.7			
	623	/		18	6.5		4	1	SE41	168	1.6		9	0.8			
SE11	106	0.5		35	29.5		37	2.3		3	1.4		37	1.5			
	3	0.6	SE22	4640	/		3	5.9		17	2.3		12	/			
	16	8.6		40	0.7		5366	/		5	16.6	SE54	91	9.4			
	153	/		2	12.4	SE33	10	1.4		300	/		6	54.5			
			SE23	904	/		4	1.2	SE42	58	10.6		24	/			

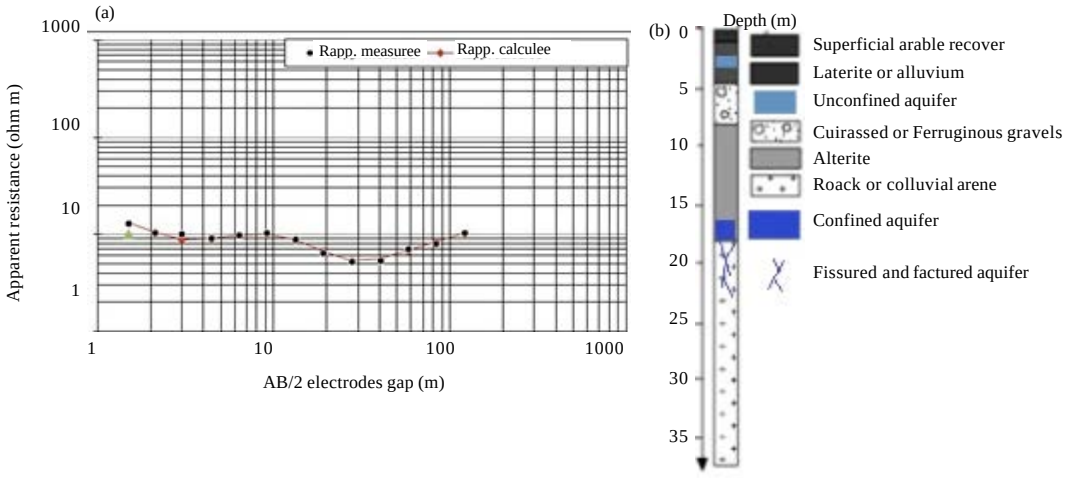

Fig. 5(a-b): Geoelectrical model and general shape of HH type curves

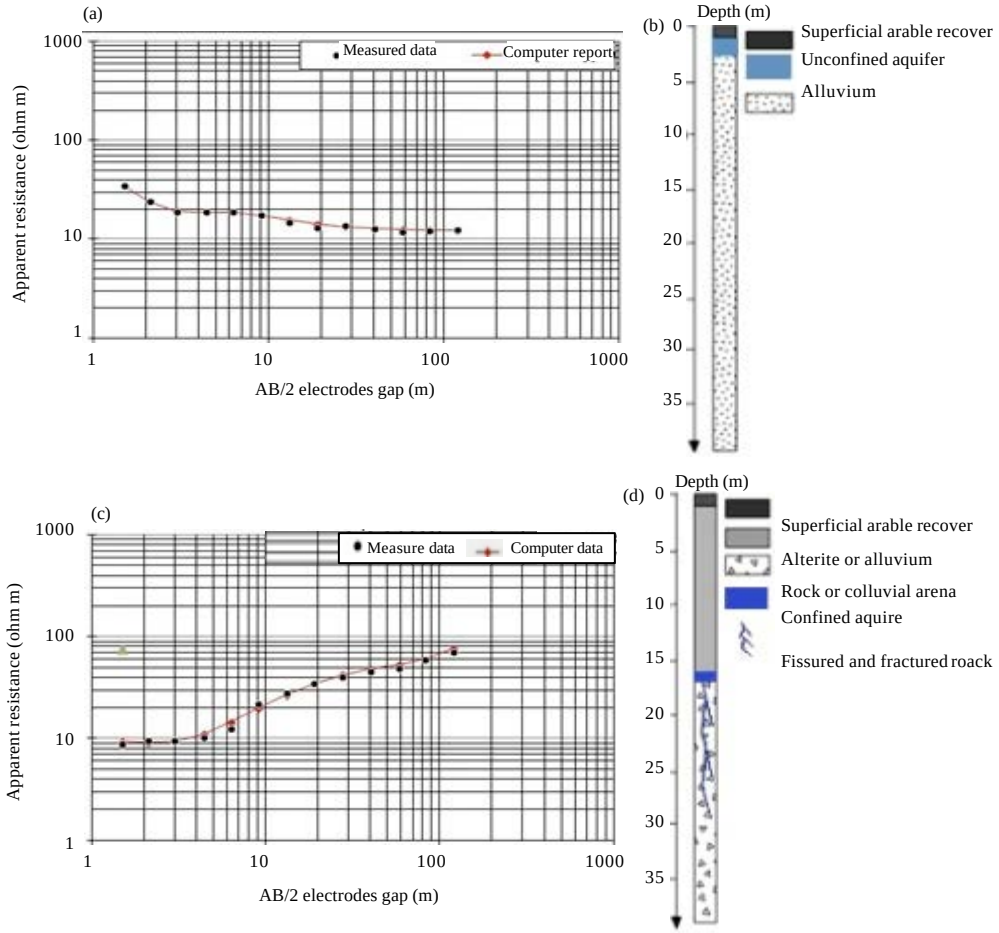

Fig. 6(a-d): General shape of A and Q type curves

Table 3: Descriptive statistics of drilling parameters

	y					
Parameters	EpAlt	Pve	EpRocksat	EpAltsat	Pt	Qest
Min	2.0	2.30	1.2	0.8	33.40	0.17
Max	64.0	27.00	24.0	45.8	89.85	9.00
Mean values	19.4	10.36	7.8	15.3	63.00	2.74
Standard deviation	13.3	7.30	4.9	10.5	12.50	2.50

Pt: Total depth of drilling EpAlt: Weathering thickness, EpAltsat: thickness of saturated weathered or alluvium layer Pve: Depth of water arrival, EpRocksat: thickness of saturated weathered Q_{est}: flow rate

Table 4: Results of correlation coefficient

Parameters	Correlation coefficient r(Q,y)
Q_{est}, Pt	-0.58
Q_{est}, EpAlt	0.32
Q_{est}, Pve	0.16
Q_{est}, EpAltsat	0.33
Q_{est}, EpRocksat	0.17

evolution and models with more terrains when they present irregularities in their evolution «drawling shape» (Table 2) (Fig. 6b, d).

In the case of type A curves, the drawling shape of the ascending slope is due to the presence of a very interesting level in hydrogeology which is made up of the fissured basement between the weathering front and the fresh basement. This curve denotes the influence of a mega fracture and presents perturbations at the level of the ascending branch. These perturbations correspond to interesting hydrogeological indices on the fractured or weathered zone of the underlying basement.

In the case of type Q curves, their drawling shape is due to the presence of a very water saturated and impermeable clayey level. The non-ascending of the curve is due to the distance of the basement which has not been attained. The profile is made up only of alluvial formations and the aquifer is very seasonal when present.

Aquifers typology: It emerges from the analysis and interpretation of electrical sounding curves figures (Fig. 3-6), two types of aquifers in this geological study area: the shallow aquifer located in the regolith and alluvium due to the presence of an impermeable sub-adjacent layer of clay with the absorbent properties that stores water, consists primarily of meteoric waters and the contributions of neighboring seasonal rivers. Although covered in some places by the cellular ironstone facies or gravelly which protects it from harsh weather conditions that influence its rechargeability, this aquifer is seasonal; the confined aquifer is developed in the gaps left by the different tectonic events which control and direct the flow of groundwater in the first 15 m of the cracked/fractured rock. This aquifer is fed on the one hand, a part of the waters of the unconfined aquifer with whom he communicates when it is existed at the top and on the other hand, through fractures connected to the drainage network rivers.

Statistical analysis and interpretation of drilling parameters based on flow rate: The flow rates obtain with the Eq. 6 and the mechanical parameters of wells varies in the general studied population (Table 3). Generally, 32 or 47% of these wells have an estimated flow rates superior to 2 $m^3 h^{-1}$ which according to Savane *et al.* (1997) is considered to be significant. About 19.12% of the flow rates are superior to 5 $m^3 h^{-1}$ and is qualified as a strong flow by the Inter-State Committee for Hydraulic Study (CIEH).

The result of correlation coefficient Eq. 10 of the different parameters individually collected with the flow rates (Table 4), show the absence of a significant relation. This is indicated by low correlation coefficient values. Nevertheless, tendencies can be cleared under certain conditions.

Total depth of drilling-flow rate relation: The relationship between the total depth of drilling and flow rate is given by the Eq. 14:

$$Y = 6.79E^{1}X^{-0.149} \quad (14)$$

For most wells, the total depth of the drill works is situated between 50 and 80 m (Fig. 7a). In this interval, more important flow rates than low flow rates are as well found. The strongest flow rates (5 $m^3 h^{-1}$) do not necessarily correspond to the highest depths. The essentials of this flow rate is situated between 32 and 65 m. However, all wells with depth beyond 75 m have flow rates lower than 2 $m^3 h^{-1}$, this seems to be an indication that, if a significant flow rate is not found beyond the depth of 75 m, it is not necessary to continue drilling. In effect, beyond a certain depth, fractures become less dense, others are closed, thus reducing the chances of meeting important flows (Lachassangne and Wyns, 2005). To this fact, Dibi *et al.* (2004), Ngo *et al.* (2010) and Koita *et al.* (2010) support the idea that, in basement contexts, the most productive wells are situated between 40 and 60 m and this depth is considered as the optimal. Generally, the maximum bored depth during

hydraulic programs is agreed upon from the start of the project, as well as a positively judged flow. When this positive flow is attained, drilling is immediately stopped without considering the possibility of finding more consequential flows at depth. On the other hand, some wells can be prolonged in the search for an imposed flow.

This explains the existence of very deep wells, due to the absence of consequential flows in the first meters. The correlation coefficient is -0.58, thus, leading to the conclusion which states that, there is no scientific consideration in the choice of well depth.

Weathering thickness-flow rate relation: The relationship between weathering thickness and flow rate is given by the Eq. 15:

$$Y = -3.26E^{-3}X^{2}+2.30E^{-1}X-4.52E^{-2} \quad (15)$$

It is difficult to clear a tendency, considering that the correlation coefficient is 0.32. If important flow rates are obtained between 18-48 m, most wells of low flow rates will equally be found in this range (Fig. 7b). At depths less than 18 m, wells of 3.5 m^3 h^{-1} flow rates do not

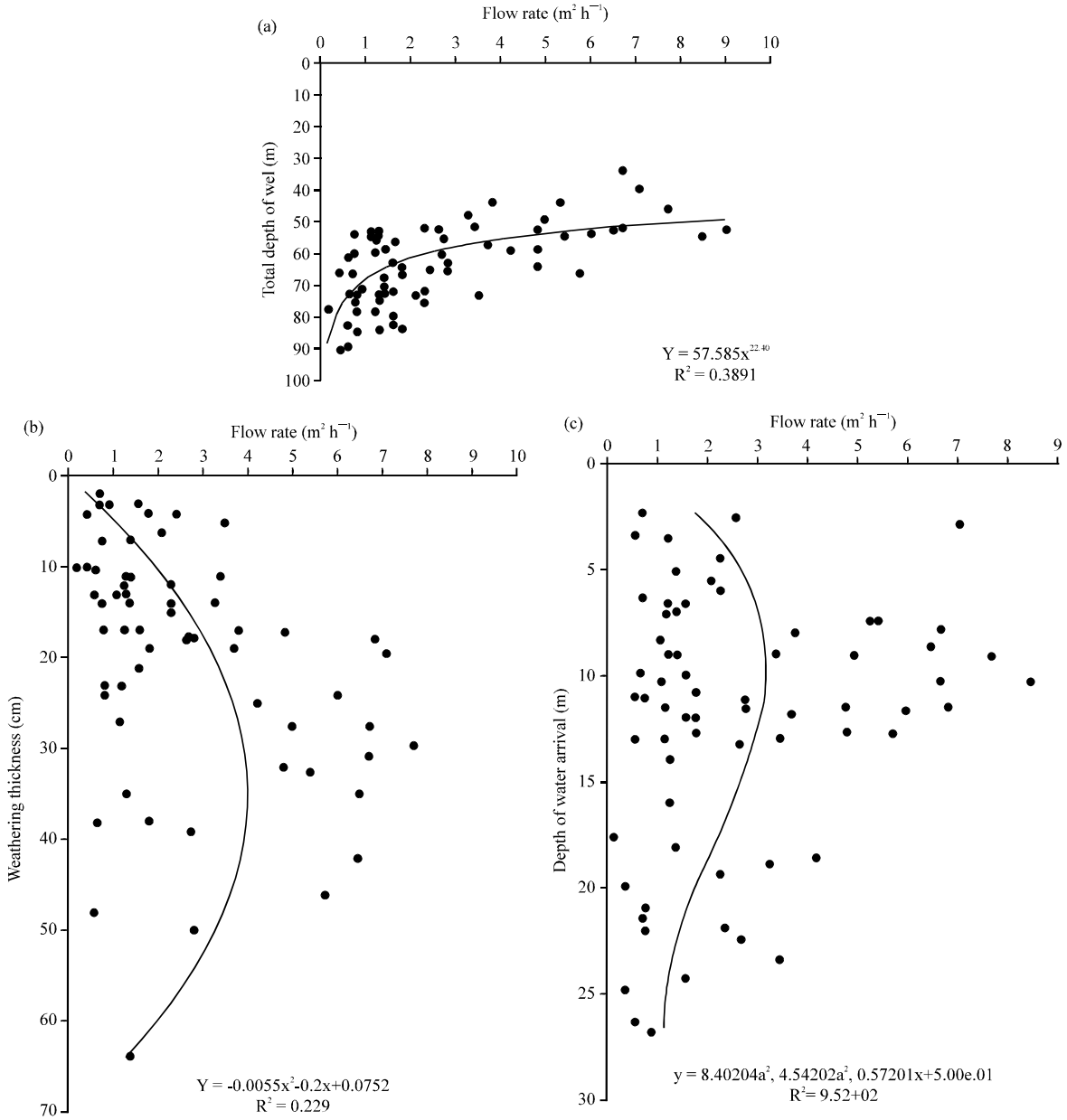

Fig. 7(a-e): Continue

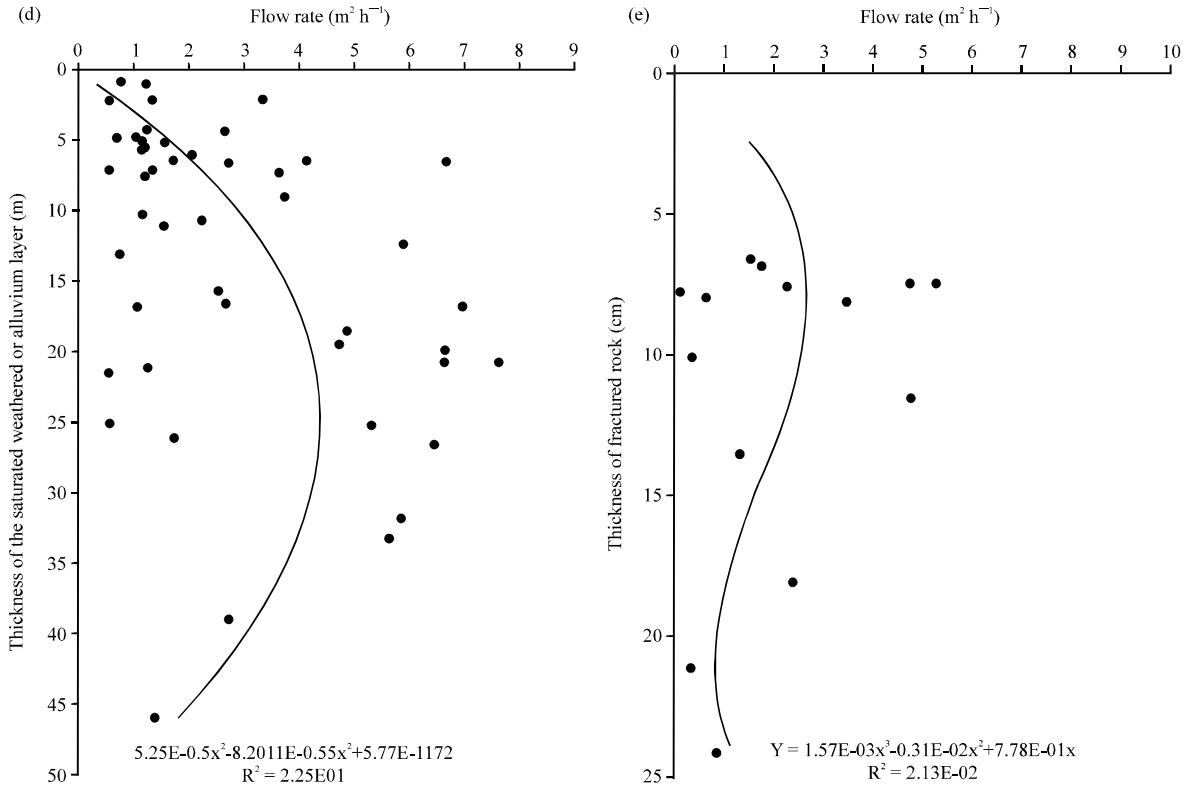

Fig. 7(a-e): Well parameter variations with respect to flow

exist. This tendency seems to tie with that verified by Koita *et al.* (2010) and Kouassi *et al.* (2012) whereby the thickness of weathered levels or alluviums increases the possibility of obtaining important flow rates. However, they precised that, this relation is not linear since it depend on the geotechnical properties of the weathered layer. As such, once the weathered layer is sufficiently thick, more than 20 m, the productivity of the well will depend on the water content of this weathering layer, its capacity to liberate its water content (porosity) and the capacity of the underlying fractures to drain the reservoir (permeability).

Depth of water arrival-flow rate relation: The relationship between the depth of water arrival and flow rate is given with the Eq. 16:

$$Y = 8.40E^{-4}X^3-4.54E^{-2}X^2+6.37E^{-1}+5E^{-1} \quad (16)$$

The distribution of points on this graphs (Fig. 7c) equally have the tendency of revealing the two types of reservoir. These reservoirs are: The superficial aquifer between 3 and 15 m, in the weathered layer and alluviums and the deep reservoir of the fissured/fractured parent rock or the underlying basement of more than 15 m. Considering water arrivals beyond 15 m to be coming from the fissured/fractured reservoir, it is revealed that, almost all flow rates above 2 $m^3 h^{-1}$ considered by Savane *et al.* (1997) as significant, are obtained from the first 15 m of the fractured rock. This tie with the earlier verification above which states that, at a certain depth, fractures became less dense and closes up, thus reducing flows in the deep fractures of the basement (Lachassangne and Wyns, 2005). Generally, the correlation coefficient is 0.16 and 0.17 in the saturated fractured rock.

Relation between the thickness of saturated weathered or alluvium layer-flow rate and thickness of fractured rock-flow rate: The relationship between the thickness of saturated weathered or alluvium layer and flow rate is given in the Eq. 17:

$$Y = 3.13\ E^{-5}X^3-8.80E^{-3}\ X^2+3.77E^{-1}X \quad (17)$$

and that between the thickness of fractured rock and flow rate in Eq. 18:

$$Y = 1.57\ E^{-3}X^3-6.81E^{-2}\ X^2+7.78E^{-1}X \quad (18)$$

From the 68 studied well, 70% captures the superficial tablecloth of the weathered or alluvium layer which presents variable thicknesses between 0.8 and 45 m.

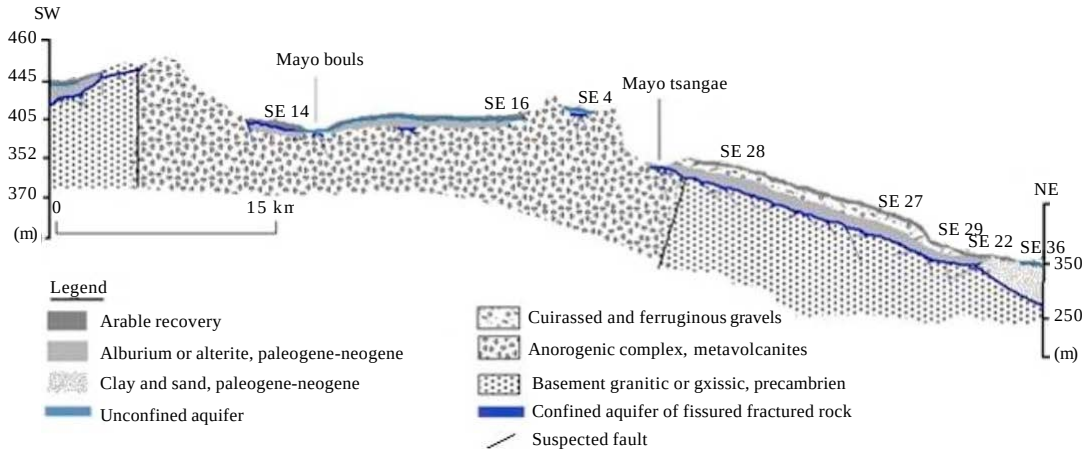

Fig. 8: Hydro-geoelectric model realized from the interpretation of electrical sounding results of piedmont region in diamare

The graphs representing the thickness of the saturated, weathered or alluvium layer with respect to flow rates (Fig. 7d), have a correlation coefficient sensibly equal to that of complete weathering (0.31). They present flow rates which increases between the thicknesses of 1-35 m and decrease for higher thicknesses. This can be due to the irregular distribution of porosity in the weathered layer or alluviums, in relation with the different phenomena of weathering and sedimentation which prevailed in the region.

It is important to note that, water arrival in wells is not only observed at the level of the saturated alterite but can also be observed in the part of the fissured/fractured parent rock. The graph (Fig. 7e) representing the depth of water saturated fractured rock with respect to flow rates, show that, the flow rate increases between 2.5 and 8 m and decreases for depths above 13.5 m. In some drill works, several water arrivals are felt in the same well, thus confirming the hydro-geoelectric models of two superposed aquifer as obtained through the interpretation of electrical sounding curves of the region and those from the works of Koussoube *et al.* (2003), Teikeu *et al.* (2012b) and Nouck *et al.* (2013).

Aquifers recharge-discharge: The Fig. 8 shows that, during rainy seasons, aquifers around the Mayos, recharge not only by rainwater through the pores and fissured rocks but also by the waters of transgression from the Mayos. However, in the dry season, under the effect of gravity and capillary aquifers lend to the Mayos, the stored water. Furthermore, this figure confirms the presence of the water, by breaking rocks in some quarries of the North-East region.

CONCLUSION

The present geophysical and statistical study was carried out in the Far-North of Cameroon, precisely in the piedmont region of Diamare. It had as aim to precise and understand the structures and functioning of aquifers and to find parameters susceptible of influencing the productivity of wells. To attain this objective, the Schlumberger sloping electrical resistivity method and statistical analyses of well parameters, were the key methods employed. As such, this study has permitted firstly from the shapes of the sounding curves:

- To identify two types of hydrogeological models, A hydrogeological model with one superficial or deep aquifer and a hydrogeological model with two superposed superficial and deep aquifer
- To localize a superficial aquifer in the weathered layer or in sandy strata of clayey alluvial episodes issued by the accumulation of eroded materials from the Mandara mountains, by the action of intense fluvio-torrential erosion and a deep aquifer in the fissured and fractured zones of the parent rock created by tectonic activity and connected to the drainage network
- To propose by intelligent modeling, an hydro-geoelectrical model of the piedmont region through the shapes of the characteristic sounding curves of soils developed in the tropical zone, where the phenomena of weathering, erosion, sedimentation and pedogenesis have printed their marks

Secondly, from the examination of graphs from the characteristic well parameters, individually collected with respect to the flow rates. These examinations lead to the following conclusions:

- The depth of a drill work is not a guaranty to an important flow in the piedmont region; beyond the drilled depth of 75 m or beyond 35 m of saturated weathered or alluvium layer, the chances of meeting an important flow rates are reduced
- The important water arrivals in deep aquifers are observed in the first 15 m of the rock
- The productivity of drill works is positively influence by the thickness of the weathered and alluvial levels but the weathered and alluvial levels has to be water saturated and sufficiently porous and permeable to liberate its water content
- The extreme variability of flows rate in the region of a borehole to another, highlighted the very discontinuous nature of these aquifers foothills
- Finally, this study has enabled to understand the aquifers recharge-discharge processes in this piedmont

ACKNOLEDGMENT

The authors thank Mrs Akozo Marie Laurence and the late Mr. Jeannot Nouck and Mrs. Julienne Ngo Matip for the financial support, assistance, general comments and suggestions. They also gratefully acknowledge Sundus Mariam and the anonymous reviewers for their detailed comments that have considerably improved this paper through their pertinent and constructive remarks.

REFERENCES

Abe-Sombo, P., F.W. Kouassi, C.S. Boko, N.L. Kouame and E.G. Kouassi, 2011. Contribution of electrical prospecting in the identification and characterization of bedrock aquifers-Department Sikensi (Southern Ivory Coast). Eur. J. Sci. Res., 64: 206-209.

Atangana, J.Q.Y., 1992. Influence of electrical and hydraulic parameters in the creation of spontaneous polarization anomalies (PS) in hydrogeology: The case of porous and fractured terrains. Master's Thesis, Blaise Pascal University, Clermont-Ferrand, France.

Biemi, J., 1992. Contribution to the geological, hydrogeological and remote sensing study of sub- Saharan watersheds of the Precambrian basement of West Africa: Hydrostructurale, hydrochemistry and isotopic aquifers discontinuous grooves and granitic areas of the High Marahoue (Ivory Coast). Master's Thesis, State National University of Ivory Coast.

Detay, M., 1987. Analytical and probabilistic identification of digital and non-digital parameters and modeling knowledge in Sub-Sahelian hydrogeological: Application in Northern Cameroon. M.Sc. Thesis, University of Nice, France.

Dibi, B., D. Inza, B. Goula, I. Savane and J. Biemi, 2004. Statistical analysis of the parameters affecting the productivity of water drilling crystalline medium and crystallophyllian in Aboisso Southeast region of Ivory Coast. Sud Sci. Technol., 13: 22-31.

Faillat, J.P., 1986. Fissured aquifers in the humid tropics: Hydrodynamics and hydrochemistry structures, (West Africa). Master's Thesis University of Montpellier, France

Koita, M., H. Jourde, D. Ruelland, K. Koffi, S. Pistre and I. Savane, 2010. Mapping of regional accidents and identifying their role in groundwater hydrodynamics in basement zone. Case study Dimbokro-Bongouanou (Ivory Coast). Hydrol. Sci. J., 55: 805-820.

Kouassi, A.M., K.E. Ahoussi, K.S.B. Yao and J. Biemi, 2012. Productivity analysis of fractured aquifers of the region Nzi Comore (East-Central-Ivory Coast). Larhyss J., 10: 57-74.

Koussoube, Y., S. Nakolendousse, P. Bazie and A.N. Savadogo, 2003. Typology of vertical electrical sounding curves for the recognition of superficial formations and their impact on hydrogeology of the crystalline basement of Burkina Faso. Sud Sci. Technol., 10: 26-32.

Lachassangne, P., N. Rampnoux, J.P. Deroin, P. Dutartre, P. Laporte and F. Mercier, 1996. Understanding of the hydrogeology of fractured base. Development methodology prospecting Town Rivers of Guyana. BRGM/Direction de la recherche, Rapport BRGM R39760 DR/HT, Pages: 96.

Lachassangne, P. and R. Wyns, 2005. Bedrock aquifers: New concept. Application for prospecting and management of water resources. Geosciences., 2: 32-37.

Meli'i, J.L., P.N. Njandjock and D.H. Gouet, 2011. Magnetotelluric method for groundwater exploration in crystalline basement complex, Cameroon. J. Environ. Hydrol., Vol. 19.

Ngo, A.Y., T. Lasm, M. Koita and I. Savane, 2010. Extraction from remote sensing networks fractures major Precambrian basement Dimbroko Region (Central East-Ivory Coast). Revue Teledetection, 9: 33-42.

Ngoupayou, J.R.N., 1997. Hydrogeochemical assessment under tropical forest in Africa: Experimental Basin Nsimi-Zoetele the river networks Nyong and Sanaga (Cameroon). Master's Thesis, University of Yaounde, Cameroon.

Nkoungou, H.L.E., P.N. Nouck, D. Bisso, S. Assembe and E.M. Dicoum, 2012. Geophysical contribution for the determination of aquifer properties in Memve Ele, South Cameroon. J. Water Resour. Prot., 4: 885-890.

Nouck, P.N., M.Y. Atangana, L. Amougou, P. Lissom and M. Yem, 2013. Geoelectrical prospection of aquifers in Eseka region, center-Cameroon. J. Emerg. Trends Eng. Applied Sci., 4: 471-477.

Pearson, K., 1895. Note on regression and inheritance in the case of two parents. Proc. R. Soc. London, 58: 240-242.

Robain, H., M. Descloitres, M. Ritz and Q.Y. Atangana, 1996. A multiscale electrical survey of a lateritic soil system in the rain forest of Cameroon. J. Applied Geophys., 34: 237-253.

Savane I., B. Goze and Q. Gwin, 1997. Evaluation of the productivity of the works in the base by studying fractures and GIS in the northwest region-Ivory Coast. Hard Rock Hydrosyst., 241: 103-111.

Seladji, S., P. Cosenza, G. Richard and A. Tabbagh, 2007. Measurement and modeling of electrical resistivity variations of a loamy soil compaction related. Proceedings of the 6th Symposium GEOFCAN Geophysique Des Sols et Des Formations Superficielles, Septembre 25-26, 2007, Bondy, pp: 75-78.

Teikeu, W.A., T. Ndougsa-Mbarga, P.N. Njandjock and T.C. Tabod, 2012a. Geoelectric investigation for groundwater exploration in Yaounde Area, Cameroon. Int. J. Geosci., 3: 640-649.

Teikeu, W.A., P.N. Njandjock, D. Bisso, Q.Y. Atangana and J.P.S. Nlomgan, 2012b. Hydrogeophysical parameters estimation for aquifer characterisation in hard rock environment: A case study from Yaounde, Cameroon. J. Water Resour. Prot., 4: 944-953.

Telford, W.M., L.P. Geldart and R.E. Sheriff, 1990. Applied Geophysics. 2nd Edn., Cambridge University Press, USA., ISBN-13: 9780521339384, Pages: 792.

Zakari, A., N.N. Philippe, E.N. Harlin, M.J. Larissa and L.T.S. Alain, 2014. Investigation of groundwater quality control in Adamawa-Cameroon region. J. Applied Sci., 14: 2309-2319.